# Numerical validation of a near-field fugitive dust model for vehicles moving on unpaved surfaces

X-L. Tong *

Center for Advanced Vehicular Systems, Mississippi State University

*Simcenter/CAVS, 2 Research Blvd, Starkville, MS 39759, USA*

*Email: xltong@cavs.msstate.edu*

*Phone number: 001-662-3253048 Fax number: 001-662-3257692*

E. A. Luke

Department of Computer Science, Mississippi State University

R. Smith

RDECOM-TARDEC, Warren, Michigan

**Abstract**

This paper presents a numerical model for evaluating fugitive dust emission and transport at near-field induced by a moving vehicle. The dust emission model describes the quantity and location of emitted dust. The transport of the dust is captured by the Lagrangian particle tracking method, and turbulence dispersion of particles is modeled stochastically. The presented model is validated

*corresponding author

# Report Documentation Page

*Form Approved*
*OMB No. 0704-0188*



| 1. REPORT DATE | 2. REPORT TYPE | 3. DATES COVERED |
|---|---|---|
| **25 SEP 2013** | **Journal Article** | **08-03-2013 to 15-08-2013** |

| 4. TITLE AND SUBTITLE | 5a. CONTRACT NUMBER |
|---|---|
| **Numerical validation of a near- field fugitive dust model for vehicles moving on unpaved surfaces** | **W56HZV-08-C-0236** |
| | 5b. GRANT NUMBER |
| | 5c. PROGRAM ELEMENT NUMBER |
| 6. AUTHOR(S) | 5d. PROJECT NUMBER |
| **X-L Tong; E Luke; Robert Smith** | 5e. TASK NUMBER |
| | 5f. WORK UNIT NUMBER |
| 7. PERFORMING ORGANIZATION NAME(S) AND ADDRESS(ES) | 8. PERFORMING ORGANIZATION REPORT NUMBER |
| **Center for Advanced Vehicular Systems,,Mississippi State University,Simcenter/CAVS, 2 Research Blvd,,Starkville,,MS,39759** | **; #24230** |
| 9. SPONSORING/MONITORING AGENCY NAME(S) AND ADDRESS(ES) | 10. SPONSOR/MONITOR'S ACRONYM(S) |
| **U.S. Army TARDEC, 6501 East Eleven Mile Rd, Warren, Mi, 48397-5000** | **TARDEC** |
| | 11. SPONSOR/MONITOR'S REPORT NUMBER(S) |
| | **#24230** |

12. DISTRIBUTION/AVAILABILITY STATEMENT

**Approved for public release; distribution unlimited**

13. SUPPLEMENTARY NOTES

**Submitted to Journal of Automobile Engineering**

14. ABSTRACT

**This paper presents a numerical model for evaluating fugitive dust emission and transport at near- eld induced by a moving vehicle. The dust emission model describes the quantity and location of emitted dust. The transport of the dust is captured by the Lagrangian particle tracking method, and turbulence dispersion of particles is modeled stochastically. The presented model is validated numerically for the prediction of dust concentration in a region near vehicles through a careful comparison to the available experimental data. The simulation results compare reasonably well with the experimental data. This model provides for the rst time, a validated dust emission and transport models suitable for the near- eld of moving vehicles.**

15. SUBJECT TERMS

**Fugitive Dust Emission, Computational Fluid Dynamics, Multiphase Flow**

| 16. SECURITY CLASSIFICATION OF: | | | 17. LIMITATION OF ABSTRACT | 18. NUMBER OF PAGES | 19a. NAME OF RESPONSIBLE PERSON |
|---|---|---|---|---|---|
| a. REPORT | b. ABSTRACT | c. THIS PAGE | | | |
| **unclassified** | **unclassified** | **unclassified** | **Public Release** | **39** | |

numerically for the prediction of dust concentration in a region near vehicles through a careful comparison to the available experimental data. The simulation results compare reasonably well with the experimental data. This model provides, for the first time, a validated dust emission and transport models suitable for the near-field of moving vehicles.

KEY WORD: FUGITIVE DUST EMISSION, COMPUTATIONAL FLUID DYNAMICS, MULTIPHASE FLOW, $PM_{10}$

## Nomenclature

| | |
|---|---|
| $EF$ | emission factor |
| $k$ | turbulent kinetic energy |
| $k_p$ | particle size multiplier |
| $M$ | surface material moisture content |
| $R_L$ | Lagrangian velocity |
| $s$ | silt content of road surface material |
| $T_E$ | Eulerian time scale |
| $T_L$ | Lagrangian time scale |
| $u$ | wind velocity |
| $u^\star$ | friction velocity |
| $\mathbf{u}'$ | turbulent velocity fluctuation |
| $\mathbf{u}''$ | random vector for turbulent velocity fluctuation |

| | |
|---|---|
| $W$ | vehicle weight |
| $x$ | vehicle travel direction |
| $y$ | cross wind direction perpendicular to $x$ |
| $z$ | vertical direction |
| $z_0$ | roughness height |
| $\gamma$ | ratio of Lagrangian time scale to Eulerian time scale |
| $\eta$ | localization factor in the localized mass injection model |
| $\theta$ | angle between point and contact point through axle on tire |
| $\xi$ | emission efficiency factor in the localized mass injection model |
| $\sigma_{\mathbf{u}'}$ | standard deviation of $\mathbf{u}'$ |
| $\sigma_{\mathbf{u}''}$ | standard deviation of velocity components |
| $\omega$ | turbulent dissipation rate |

# 1 Introduction

Particles suspended in air by vehicular movement on paved and unpaved roads are a major contributor to fugitive dust emissions, which in turn can have significant impact on many aspects of vehicle performance. Scattering caused by suspended dust particles and dust deposition on wind shields and mirrors can impair visibility, especially in convoy types of settings. Operationally, dust can be ingested by the engine and power

train, increasing maintenance expense and reducing vehicle life-time. In commercial applications, the transport of particulates around a vehicle is of particular interest in determining vehicle soiling. Therefore, accurate prediction of dust emission and transport in the near-field of moving vehicles is needed to evaluate the impact of dusty environment on many aspects of vehicle performance.

The following sections start with the literature review on the current status of the research on emission and transport of fugitive dust. It is then followed by our methodology which includes the development of specialized models for emission of particles and their transport and dispersion by the turbulence in the vehicle wake and atmospheric boundary layer (ABL). Finally, A careful comparison between the numerical model and experimental data is presented, providing one of the first attempts at validating a numerical model for the near-field dust transport around a moving vehicle.

# 2 Literature Review

There are a number of challenges involved in the modeling of dust emission and transport caused by moving vehicles traveling on unpaved roads. The dust generation mechanism is dependent on complex phenomena that occur at the contact between the vehicle tires/treads and the dusty surface. The amount of the dust emission depends on many factors such as dust particle properties (size, density, stickiness, etc.), environment conditions (wind speed,etc.), soil conditions (silt content, moisture level, etc.) and vehicle features (vehicle velocity, weight, dimension, number of the wheels, etc.). There have

been many experimental investigations of the relationship between the magnitude of dust emission and the above factors. Experimental methods include upwind-downwind method [1, 2, 3], exposure profiling method [4, 5], filter-based gravimetric techniques [6, 7], field wind tunnel [8, 9, 10] and the optical remote sensing method [11]. The U.S. Environmental Protection Agency (EPA) has collected and compiled the dust emission factor data gathered in various field studies over last few decades. The data and dust emission models are documented in the *Compilation of Air Pollutant Emission Factors* (AP-42) [6, 7, 12]. It has to be mentioned that most experimental work on dust emission induced by vehicles has the objective to model dust emissions as line sources for air quality modeling, and thus near-field collection of data was not the priority. As for modeling of dust emission and transport in the near-vehicle region there has been relatively small amount of work described in the open literature. Chen et al. conducted near-field work on real-time realistic visualization of vehicles [13, 14]. The numerical model aimed at representing vehicles in a virtual environment and a computationally efficient model was needed since interactive graphics required the model operate faster than physical time. As a result, their numerical models were highly simplified, and the simulation results were not validated by any experimental study.

Turbulence provides another challenge in the modeling of dust transport around the vehicle. Once emitted in the air, the dust is scattered by small scale turbulent eddies that form in the vehicle wake as well as large scale turbulent eddies that are superimposed from the ever present ABL. There has been a number of research on the

particle dispersion modeling in the fields of air quality control. The dispersion models include Box models [15], Gaussian models [16] and computational fluid dynamics (CFD) models [17]. In Box models, the air is in the shape of a box and the air mass is assumed to be homogeneously distributed inside the box. This model is very limited in predicting the particle concentration, especially in a local environment due to the simple uniform particle distribution assumption. Gaussian type models are most commonly used in atmospheric dispersion modeling. It is based on a Gaussian distribution of the plume in the vertical and horizontal directions, and the width of the plume is a semi-empirical function of the atmospheric stability class [18]. Gaussian models can also be used for predicting the dispersion of non-continuous plumes by emitting a series of puffs over time and super-imposing the particle concentration fields associated with each individual puff [19]. Gaussian models are normally applied for modeling the particle dispersion in atmosphere in the far field, and restricted to the sites close to the source. CFD models compute the solution of the complex flow field based on conservation of mass, momentum and energy by solving Navier-Stokes equation. Turbulence is modeled by various closure models [20]. Holmes et al. provided a comprehensive review of different dispersion models and their applications [21]. The review showed the considerable difference between the available dispersion modeling packages and their limitations.

# 3 Numerical Simulation Models

The verified production Loci/CHEM multi-physics CFD code [22, 23] was utilized to simulate the dust emission and transport around a moving vehicle in this study. The CHEM code is developed under the Loci framework[24], and it is a robust, highly parallel solver that provides a variety of turbulence models and Lagrangian particle models that are needed to model the physics of dusty flows.

In the present simulations, The turbulence in ABL was modeled by engineering level RANS based turbulence model. Special care must be taken to ensure that the ABL is sustained over the simulation domain. The failure of RANS based models without proper treatment to accurately capture the ABL has been described in the literature[25, 26, 27]. In the simulations, the method proposed by Richard and Hoxey [28] was adopted whereby the ABL is sustained by utilizing an appropriate surface roughness parameter on the ground along with an imposed stress boundary condition on the upper boundary. This scheme was implemented within Menter's baseline (BSL) turbulence model [29]. In a separate study [30] it was found that the approach is effective at maintaining the ABL over the domain sizes considered in this study which are on the order of a few dozen vehicle lengths.

The Lagrangian particle tracking method was employed to compute the transport of the fugitive dust emissions. Since the RANS turbulence models do not resolve the turbulent eddies, the Lagrangian particle tracking method will not recover the dispersion that these eddies cause. In order to correctly reconstruct the scattering effects

of the modeled turbulent eddies, A stochastic model of the turbulent fluctuations was employed [31, 32, 33]. In particular the method of Zannetti[34] was used whereby the turbulent velocity fluctuations, $\mathbf{u}'$, were modeled as a simple first order auto-correlation Markov process. In this formulation, turbulent fluctuation, $\mathbf{u}'$, is expressed as

$$\mathbf{u}'(t_2) = R_L(t_2 - t_1)\mathbf{u}'(t_1) + \mathbf{u}''(t_2) \tag{1}$$

where $R_L(t_2-t_1)$ contains the auto-correlation with lag $\Delta t = t_2-t_1$ of the $\mathbf{u}'$ components where $\mathbf{u}''$ is a purely random vector. Using this method the perturbation of each particle is independent and not affected by the position of other particles in the flow. Therefore, the numerical performance is fast since no special interactions between particles and fluid are required. The auto-correlation of the Lagrangian velocity, $R_L$ can be related to Lagrangian time scales, $T_L$ by $R_L = exp[-(t_2 - t_1)/T_L]$ where Lagrangian time scale represents the time over which the velocity of a particle is self-correlated. There is another time scale - Eulerian time scale ($T_E$) that represents the time the turbulent eddy pass through a fixed point and it can be derived from the energy dissipation time scale. Normally Lagrangian time-scales are more difficult to measure and are often related to the Eulerian time scales through the relation $T_L = \gamma T_E$ [35, 36, 37]. In current study, $\gamma$ was chosen to be unity according to other experimental result [35]. Assuming that turbulence is homogeneous and isotropic, the Eulerian time scale can be determined from the RANS model using the relation $T_E = \frac{1}{3}\frac{2}{C_\mu \omega}$ where $C_\mu = 0.09$. The specific dissipation rate variable, $\omega$, is a scalar field obtained from the turbulence

model. The assumption of homogeneity is satisfactory for near-field simulations. In case of the inhomogeneity of turbulence in longitudinal, lateral, and vertical directions for more distant atmospheric transport, the 1/3 factor is replaced with an appropriately weighted set of coefficients for each of the corresponding directions.

Next term to be modeled in equation(1) is the random vector $\mathbf{u}''$. It is assumed that $\mathbf{u}''$ follows normal distribution of $\mathbf{u}'' = \frac{1}{\sqrt{2\pi\sigma_{\mathbf{u}''}}} exp(-\frac{x^2}{2\sigma^2_{\mathbf{u}''}})$ where $\sigma_{\mathbf{u}''}$ is the standard deviation of the velocity components, characterized by $\sigma_{\mathbf{u}''} = \sigma_{\mathbf{u}'}\sqrt{1 - R_L^2(t_2 - t_1)}$ where $\sigma_{\mathbf{u}'}$ is the standard deviation of $\mathbf{u}'$, defined as $\sigma_{u'} = \sqrt{\frac{2}{3}k}$ where $k$ is the local turbulent kinetic energy.

# 4 Modeling Dust Emissions

For the purpose of simulating the near-field dust emissions, models are needed to describes the amount of dust emitted, the emission location on the tires/tracks, and the particulate size distribution. The overall mass flux of particles emitted from a moving vehicle has been relatively well characterized by a number of studies[7, 1, 2, 3, 38, 39, 40] which describe the total emissions from vehicle traffic (suitable for use in line source models) based on various factors such as vehicle speed and weight, soil silt content, and soil moisture content. These studies do not provide localized information about the distribution of dust, however studies have shown that the total mass of dust smaller than $10\mu m$ remains relatively unchanged over distances on the order of 1 kilometer provided that the terrain is relatively open[3]. The downwind dust emission measure-

ments in emission models are usually made 5 meters from the road. For air quality modeling the EPA model AP-42[12] is the most widely used emission model to quantify particle emission due to vehicle traffic on unpaved roads, even though there are some criticism of this model for lacking mechanistic foundation [41]. Since there is no better available model, the AP-42 model was adopted to characterize the bulk mass flux of particle emissions. This global model was combined with localized mass injection formulation to construct a near-field dust emission model. The components of this model are outlined in the following subsections.

## 4.1 The EPA AP-42 Model

The AP-42[12] models were developed using multiple linear regression analysis of emission factor (EF) test data versus parameters that affect the amount of particle emissions. Although the emission factor model for unpaved road has been modified over the past 20 years, all versions have important common features. The silt loading has consistently been found to be the most important factor in emission models. In this study, the 2003 version of AP-42 emission factor model was adopted. It was developed through a collection, selection and analysis of data from 12 field test reports on dust emission induced by vehicles traveling on unpaved roads, as shown in eqn. (2).

$$EF = \frac{k_p(s/12)^a(W/3)^b}{(M/0.2)^c} \tag{2}$$

Table 1: Parameters for eqn. (2)

| constant | $PM_{2.5}$ | $PM_{10}$ | $PM_{30}$ |
|---|---|---|---|
| k | 0.38 | 2.6 | 10 |
| a | 0.8 | 0.8 | 0.8 |
| b | 0.4 | 0.4 | 0.5 |
| c | 0.3 | 0.3 | 0.4 |

where $EF$ = Emission factor, pounds per vehicle-mile-traveled, (lb/VMT)

$k_p$ = Particle size multiplier (dimensionless)

$s$ = Silt content of road surface material (%), which refers to portion of mass of silt-size material (equal to or less than 75 $\mu m$ in physical diameter) per unit area of the travel surface

$W$ = Mean vehicle weight (ton)

$M$ = surface material moisture content (%)

For air quality purposes the particulate emissions are characterized into three size classifications of particle matter (PM) known as $PM_{30}$, $PM_{10}$, and $PM_{2.5}$ which represent all particle matter that has an aerodynamic diameter less than $30\mu m$, $10\mu m$, and $2.5\mu m$ respectively. Aerodynamic diameter is the diameter of a sphere of unit density ($1000kg/m^3$) that has aerodynamic behavior (e.g. settling velocity) identical to that of the particle in question, thus the actual shape or density of the particles is not of concern. The particle size multiplier, k for different size range for eqn. (2) is given in table 1.

Note that "normalizing factors" of 12% silt content and 3 kilogram vehicle weight are used in the model. The soil moisture content of 0.2% is selected as the reference moisture which is usually considered as the default dry condition moisture content. A summary of values of silt content on industrial and public roads was given by the table 13.2.2-1 in AP-42 [12]. Mean silt contents for gravel roads and dirt roads are found to be 6.4% and 11% respectively. The moisture content is influenced by meteorological and physical parameters that varies with time and location. According to AP-42, the overall mean moisture content in publicly accessible road data set was 1.1%. The moisture content for the desert ranges from 0.17% to 0.48%. Vehicle weight ranges from 1.5 ton to 244 ton in the collected field data. Note for these models to remain consistent with experimental conditions, mean wind speed should range between 4 to 20 MPH ($1.78m/s$ to $8.89m/s$), and wind direction is within 45° perpendicular to the road.

## 4.2 Localized Mass Injection Model

The EPA AP-42 model provides a reasonable estimation for the bulk of particulate matter that is emitted due to vehicle travel (at uniform speed on a unpaved road surface). However it provides no information about where the emissions emanate from a vehicle. In current simulations the detailed transport of particulate matter around the geometry of the vehicle was of interest and therefore information on the actual locations of emissions was desirable. Generally emissions come from three sources: 1) directly

from the contact points (e.g. tires or tracks) of the vehicle with the dusty surface, 2) saltation processes caused by impacts of emitted particles with the surface, and 3) particles liberated due to the action of shear of the air flow created by the vehicle motion. For dusty unpaved road surfaces it is assumed that the majority of dust is emitted directly from contact points rather than from saltation and shear processes, which appears to be the case from simple observation of vehicles traveling on unpaved roads.

For the contact point emissions, there appears to be two primary mechanisms for emission: 1) surface adhesion and shear with the ground cause particulates to stick to the tire/track which are then emitted due to centrifugal force as the tire/track rotates up from the ground, and 2) crushing action at the leading edge of the tire/track causes particles to be ejected at the leading edge. Unfortunately, there has been no published experimental data that provides localized information on emissions such as the relative quantity of particulate matter emitted from these localized regions. Despite of the lack of quantitative data, a model was created in current study that qualitatively produces dust plumes near the tires that is consistent with the observation.

In the emission model it is assumed that emissions come from the tire/tread surface and a probability of emission as a distribution over the tire is assigned. A schematic diagram shown in figure 1 describes the tire contact with the ground. An emission probability is computed based on the angle of the tire tread surface normal with respect to the coordinate system formed by the axle vector (into the page) and the gravitational

force vector. If the surface normal points within 10 degrees of the axle vector, it is assumed that this is part of the tire sidewall and the emission probability is set to zero. Otherwise the probability is set by the angle $\theta$ as shown in figure 1. The non-normalized emission probability is given by the equation

$$\xi = \epsilon * (\max\{\cos\theta, 0\})^{\eta} \tag{3}$$

where $\epsilon$ is an efficiency factor that scales the emissions between the leading and trailing points of contact, and $\eta$ is a parameter that describes the localization of emissions. The maximum function prevents emissions from occurring on the top of the tire. The efficiencies, $\epsilon$, and localization parameter, $\eta$. for the trailing contact point (where $\theta$ is positive) are set to $\epsilon_t = 0.9$ and $\eta_t = 2$, while for the leading contact point (where $\theta$ is negative) they are set to $\epsilon_l = 0.1$ and $\eta_l = 6$. With these settings, 90% of the emissions come from the trailing point of contact, while the emissions from the leading point of contact has a distribution heavily biased towards the ground region. Particles are ejected from the trailing edge with the tire velocity, while at the leading edge the sign of the velocity is reversed such that the particles are emitted into the incoming flow and re-entrained into the wake flow. The probability distribution function is formed by normalizing $\xi$ by the integration of $\xi$ over the tire surface. Particles are assumed to be emitted from the surface with the tangential velocity of the rotating tire. This model was utilized to describe where the particles are emitted from, while the overall mass flux was adjusted to meet the AP-42 model for vehicle dust emissions.

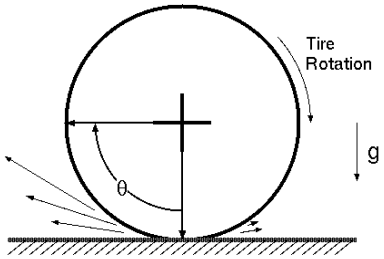


Figure 1: Schematic of Tire-Ground Contact

# 5 Qualitative Evaluation

Before validation study on the model, A simulation of dust distribution around a moving vehicle was performed to determine if the model produced qualitatively reasonable results. For this test a Nissan Pathfinder SUV was chosen since its geometry was already available to evaluate the simulation of dust transport for a realistic configuration. A viscous mixed element mesh with 15 million cells was generated by the SolidMesh/AFLR3 mesh generation software[42].

For the simulation of particle emission and transport, the SUV traveled at 13.5m/s (about 30MPH) uniform forward velocity with a cross wind of 6.75 m/s (about 15MPH). The wind was simulated as an ABL with a velocity of 6.75m/s at one meter height using a surface friction velocity of $u_\star = 0.6m/s$ and roughness length of $y_0 = 0.01m$. The rubber part of the tire was prescribed a rotational velocity 348.42 RPM which was consistent with a forward velocity of 13.5m/s. The rotation of the spokes of the hub was not considered in this model. Particles having material density of quartz (2648

$kg/m^3$) were emitted using log-normal particle size distribution with particle median aerodynamic diameters of $30\mu m$ and a variance of 0.25. The BSL turbulence model and the first order stochastic turbulent dispersion model were employed in the simulation. Initial dust mass flux released by tires was determined using the model described by eqn.(2). The silt content and soil moisture content were set to the default value, namely 12%, and 0.2% respectively. The weight of vehicle was taken from Nissan Pathfinder, which is $4500kg$. The mass flux computed from the model was equally distributed to the 4 wheels. Particles were ejected from the tires using the localized mass injection model represented by eqn.(3).

Side and top views of the simulated dust distribution around the vehicle for this case are shown in figure 2. Instead of viewing particles as points, the volume visualization method was used in which the computed particle concentration field was averaged over the volume in time allowing the particle cloud to be viewed as a semi-transparent region to mimic the scattering effects that visually dominate particle plumes. From this figure it can be seen that the localized release model of particles produces a distribution of dust both around the tires and the vehicle that follows qualitative expectation. Particles are initially released near the tire contact points and are then entrained by the recirculating flows in the vehicle wake and scattered by both the wake and atmospheric turbulence. The structure of the mean wake of the vehicle is not strongly evident because turbulent dispersion plays a role in scattering the particles. Note that since the stochastic model does not include any spatial correlations, there is no billowing type of effect. Each

particle follows its own "Brownian Motion" type of trajectory, but a group of particles in the same region of space do not follow the same "eddy" and the overall effects are averaged out to give an average characterization of the particle plume. In general, these results show that the described model performs in a fashion that is qualitatively comparable to the observed dusty cloud produced by vehicles traveling on unpaved surfaces.

Figure 2: Dust distribution around the moving vehicle from views on front driver's side (top), front passenger side (middle) and top (bottom) with volume visualization

# 6 Model Validation Case

In order to validate the model in the near-field, it is desirable to compare the simulation results to the experimental data that is as close to the vehicle as possible. Unfortunately, most experimental data were collected at some distance from the vehicle since their purpose was to validate environmental quality models that treated dusty roads as line sources. Through the review of the available literature, it was determined that measurements of dust concentrations carried out by Veranth *et.al* [3, 43] provided the most appropriate data for our validation needs. The main reason this data set was chosen is that the measurement data were conducted at 3 meters away from the road, while other measurement results were performed at much greater distances. In addition, the data presented in these experiments included absolute measurements of dust concentrations that were suitable for validation exercises, instead of relative measurements that were designed to calibrate existing models. Finally, compared to other experimental work, the running conditions in this field study were relatively well documented which makes this data set more suitable for the model validation.

## 6.1 Outline of Experimental Data Set

The field measurements were conducted at the Dugway Proving Ground, Tooele County, Utah by University of Utah in collaboration with the Mock Urban Setting Test(MUST). The original purpose of this study was to investigate the significance of near-source removal of the dust under the stable atmosphere and high surface roughness conditions.

Surface roughness that might be presented by large surface roughness like buildings was modeled in the experiment by a 10 by 12 array of 2.5m high, 2.4m wide, and 12.2 long rectangular cargo shipping containers. In the surrounding landscape, vegetation was a thin cover of brush of 0.5-1m high. The soil was classified by the Natural Resources Conservation (2000) as Skumpah silt loam with 16% silt content. The atmospheric condition was stable. The background dust concentration without vehicle traffic was $10\mu g/m^3$ and thus negligible since it was at least 3 magnitude lower than measurements with vehicle activities. The test was performed using a 1994 Ford pickup truck with $3900kg$ weight that was driven at the speed of $9m/s$ on an $180m$ long unpaved road that ran parallel to the upwind edge of the container array. Wind speed was normally between $1m/s$ and $5m/s$ and the wind direction remained within 45° perpendicular to the road. Average air temperature and pressure were $294K$ and $0.855atm$ respectively.

Dust concentration was measured using DustTrak analyzers with $PM_{10}$ inlets. The instruments were mounted on a movable tower at various heights to collect the data at different location. As the near-field predictions were of interest, only the measurements by the near-source tower which was located 3 meters from the edge of the road, or 4.5 meters from the road center-line were considered in validation study. Dust measurements were performed on the tower at heights of 0.9, 1.7, and 3.7 meters above the ground. The vehicle was traveling for total 1.5 hours as a series of 44 trips at 1-1.5 minute intervals, and the time-averaged dust concentration was recorded every 5 seconds. Peak concentration value for each trip ($mg/m^3$) and pulse area defined as the

time integrated concentration per trip ($mgs/m^3$) were recorded in the experiment and are provided in table 2.

Table 2: Mean and standard deviation of dust concentration data at near-source (3 meters from the road)

| Height(m) | peak concentration ($mg/m^3$) | pulse area ($mgs/m^3$) per trip |
|---|---|---|
| 0.9 | $38.9 \pm 21$ | $302 \pm 171$ |
| 1.7 | $19.9 \pm 11$ | $144 \pm 92$ |
| 3.7 | $10.3 \pm 7.2$ | $77.8 \pm 56$ |

## 6.2 Simulation Setup

For the simulation setup simulations were performed in the vehicle reference frame. In this reference frame, the tower moved through the domain at the rate of the vehicle speed, and the time history of the particle concentrations can be obtained by plotting the concentrations along a line that represents the measurements at a given tower height. Therefore distance along the line can be converted into time in the tower's reference frame simply by dividing by the vehicle speed. Thus a straightforward way was available to compare simulation results to measured experimental data provided that the simulation domain is large enough that the entire pulse of the particle plume was recorded within the domain. The first step in this process was the generation of a mesh for a long domain that included the vehicle and enough downwind region to properly simulate the plume's intersection with the measurement tower. In the experiment, a 1994 Ford Pickup truck was used as the dust emission source. For the

geometry of the 1994 Ford Pickup a simplified model was constructed based on general vehicle geometry available in generic descriptions from Ford including vehicle wheelbase, bed dimensions, and cab height. Figure 3 shows the resulting simplified pickup truck geometry. To determine the sensitivity of the dust plume at the first tower location to the vehicle geometry, simulations were conducted using the detailed Pathfinder SUV and the approximate pickup truck geometry and it was found that there were not significant differences in the simulated dust distribution at the tower location 3 meters from the road. This was not surprising as it confirmed the observations in the work of Gillies *et.al* [1] that showed that the size of the wake created by a moving vehicle was mainly dependent on the height of the vehicle. In the current study, the heights of SUV and pickup truck were about the same, namely 1.7m and 1.9m respectively. From these studies we concluded that the simplified geometry of the pickup truck was sufficient for validating to the tower data that is 3 meters from the edge of the road. A viscous mixed element mesh containing 5.4 million cells was generated in the computational domain.

The experimental data setup used for validation included an array of cargo containers that were placed about 6 meters from the road with the first dust tower being just 3 meters away from the road edge. Although the dust tower is upwind of the container array, the effect of the blockage represented by the container array will cause an uplifting flow caused by the blockage of the array. To correctly capture the effects of the container array in our validation, a rectangular block was created with the same height

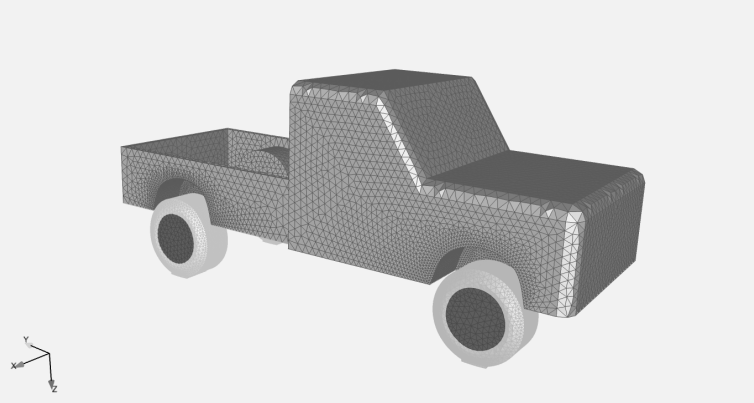

Figure 3: Geometry and surface mesh of a Ford Pickup truck

of the containers ($2.5m$) located at $6m$ from edge of the road (distance was estimated from the schematics given in the Veranth's paper [3]) and extended along the road throughout the domain as shown in figure 4. Comparison of dust plumes from the simulations with and without this blockage showed that it contributes a significant effect in the height of the dust plume at the closest measurement tower. In current simulation the container array was simplified as if it was a continuous obstruction along the road which approximates the blockage effect of the containers while also facilitating a simple steady-state simulation procedure.

Empirical evidence suggests that in the near-field only a very small amount of particles will be removed from the domain by way of deposition. Therefore, it was assumed that no particle deposition occurs and any particle that interacts with the vehicle or ground surface rebounds specularly off of the surface. For simulations over larger dis-

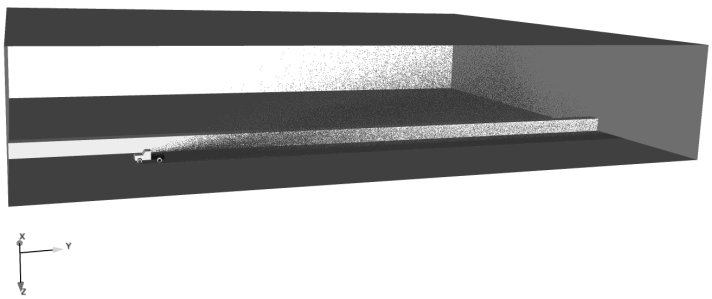

Figure 4: Computational domain with a blockage parallel to the vehicle traveling direction. White-gray rectangular part is the blockage, and particles are represented by black color.

tances, a proper ground deposition model may be required to properly consider ground particle interactions.

Dust with material density of quartz was emitted from the tires with a distribution that is described by eqn.(3) with the mass emission equally distributed to the four tires. The total mass flux of the tire emissions were determined by the AP-42 model as described by equation(2). The parameters of 16% silt content, $3900kg$ vehicle weight, 0.2% moisture content with particle size multiplier from $PM_{10}$ were input to the eqn.(2) to get dust emission factor. This value combined with the vehicle speed of $9m/s$ gave $0.0096kg/s$ total mass flux injected from four tires. The distribution of the particle sizes was prescribed by a log-normal distribution with a median particle physical diameter of $2.5\mu m$ with standard deviation of 0.35. This distribution covers physical diameters less

than $6.1\mu m$ (corresponding to aerodynamic diameter of $10\mu m$) with the similar mass emission ratio between $PM_{10}$ and $PM_{2.5}$ in eqn.(2).

To simulate the atmospheric wind effects, a background atmospheric wind profile was prescribed using logarithmic law as $u = \frac{u^\star}{K} ln(\frac{z+z_0}{z0})$ where $K = 0.4$, and friction velocity ($u^\star$) and roughness height ($z_0$) were estimated to fit the upwind data within the variation of measurements in the field study. $u^\star$ of $0.24m/s$ and $z_0$ of $0.01m$ were selected in the wind profile expression. The value of friction velocity agreed very well with field measurement of $u^\star$ from sonic anemometer data ($u^\star = 0.23m/s$). Figure 5 demonstrates that the prescribed wind speed profile compared well with experimental data. As mentioned in field study, wind direction was within 45° perpendicular to the road, but there was no data on average wind direction. In our simulation, the wind direction was first set perpendicular to the road, then 45° to the road to evaluate the bounding effects of wind direction in the validation.

## 6.3 Validation Results

Simulations for two different wind directions (90° and 45°) were conducted for comparison to experimental data at the closest tower location. The dust concentration temporal history for each of the three tower sampling heights (0.9, 1.7, and 3.7 meters) was determined from the steady state simulation. These tower heights are represented in the figure 6 showing three lines that represent the three sampling heights drawn on a cutting plane located at the tower location. From these spatial lines a temporal history

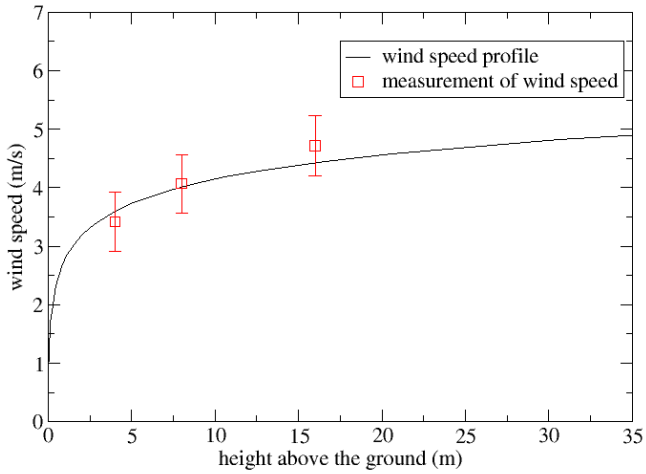


Figure 5: Comparison of prescribed atmospheric boundary layer profile and experimental data with variation of measurement

can be reconstructed as shown in figure 7. The peak and integrated concentrations of particles at each of the tower heights were determined for comparison with experimental data as shown in table 3.

The simulated peak dust concentration compared reasonably well with experimental data and were generally with experimental error bounds. Note that the wind direction used in the simulation had a significant impact on the resulting dust distribution at the tower location. In general, the simulations at the larger wind angle were more consistent with the experimental data, and the simulations appeared to under-predict integrated dust concentrations suggesting that perhaps more particles should have been emitted from the vehicle tires. In addition, it appeared that the experimental results showed a slightly more dispersed particle plume than the simulation, in particular when comparing the integrated particle concentrations at the highest tower sampling location. However, the simulations were still within the experimental error bounds and so no definitive conclusion can be made. From these simulations, it was also clear that the wind characterization was a significant source of variability in the measured and simulated data, thus contributes uncertainty in the process of validation/calibration.

As already mentioned, numerical studies showed that details of the vehicle geometry did not play a significant factor in the measured dust plume. In addition a number of additional simulations were performed to determine the effect of other factors that may affect comparisons to the numerical experiments. The first consideration was the effects of the size distribution of the emitted dust particles. For the dust size distribution the

Table 3: Comparison of dust concentration results between CFD simulation and experiment at closest tower (3m from road) with perpendicular and 45° simulated cross winds

| Height (m) | measured peak concentration ($mg/m^3$) | simulated peak concentration ($mg/m^3$) | | measured pulse area ($mg\ s/m^3$) | simulated pulse area ($mg\ s/m^3$) | |
|---|---|---|---|---|---|---|
| | | 90° | 45° | | 90° | 45° |
| 0.9 | $38.9 \pm 21$ | 51.8 | 27.5 | $302 \pm 171$ | 124 | 106.2 |
| 1.7 | $19.9 \pm 11$ | 49.0 | 25.6 | $144 \pm 92$ | 120.8 | 90.4 |
| 3.7 | $10.3 \pm 7.2$ | 10.1 | 7.75 | $77.8 \pm 56$ | 15.2 | 29.3 |

amount of dust in the different categories can be inferred from the EPA model which provides different coefficients for $PM_{2.5}$, $PM_{10}$, and $PM_{30}$ dust size categories. An exponentiated Weibull size distribution PDF was derived based on the coefficients for different sizes in EPA model. Comparison was made between simulations using log-normal (as used in the presented results) and the exponentiated Weibull distribution with cut-off aerodynamic diameter of $10\mu m$. Same amount of the dust was released from the tires in both simulations. It was found that there was no significant difference in the measured dust plume between these two PDFs suggesting that particle sizes play a minor role in the plume dispersion at the nearest tower. In addition, the effect of the exponent on the localized dust emission model given in eqn.(3) was evaluated by comparing a linear distribution ($\eta = 1$) instead of the square law used in the validation study. In terms of the plume shape observed at the 3 meter tower location, changes in the tire release model did not significantly change the dust distribution. However, the exponents used in the study produced a dust plume that better matched the qualitative

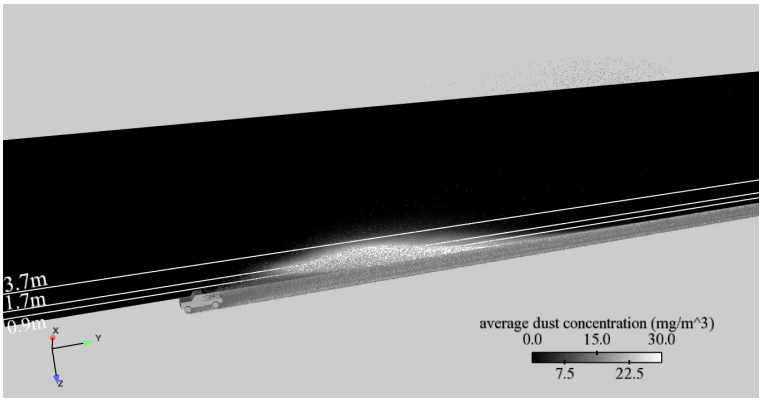


Figure 6: Dust distribution on the near-source plane (3m from the road, 90° wind)

character of tire emissions observed from vehicles moving on dusty roads.

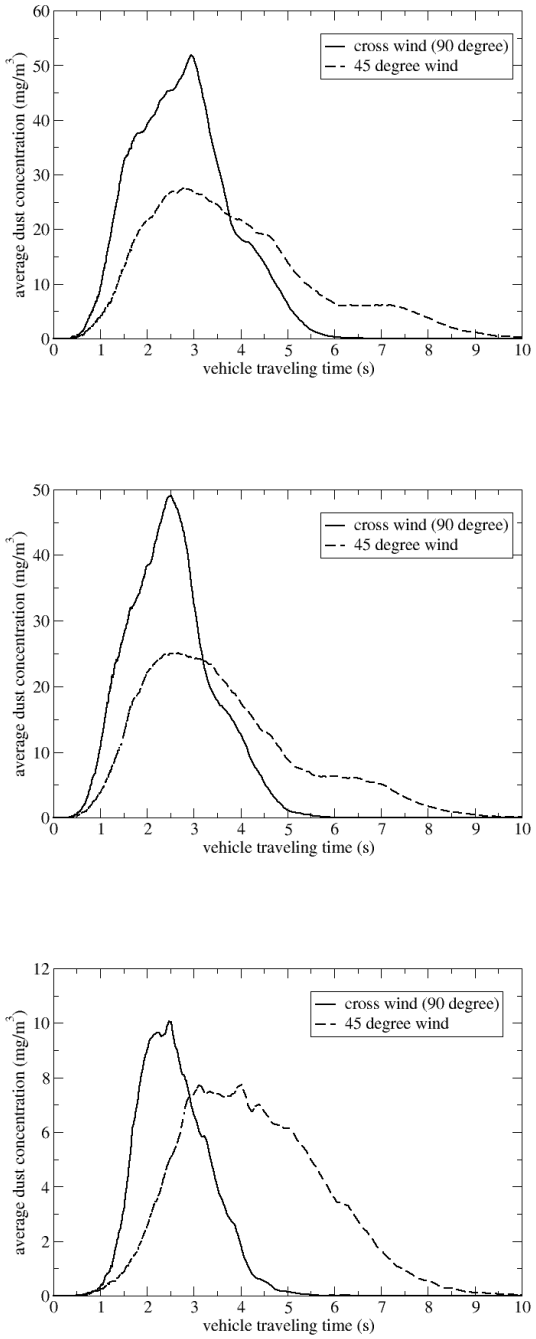


Figure 7: The simulated dust concentration pulse for different wind direction at 0.9m (top), 1.7m (middle) and 3.7m (bottom) measuring stations.

# 7 Concluding Remarks

Many aspects of vehicle functionality depend on the emission and transport of fugitive dust caused by vehicle movement, especially when traveling on unpaved surfaces. Given the needs for particle emission models, there are very few detailed models of the fugitive dust in the vehicle near-field region. This paper presented a modeling approach for fugitive dust emission and transport that can capture near-field dust concentrations. The model was validated by comparing simulated dust plumes with experimental data at 3 meters from the edge of the road. It was found that the proposed model performed within experimental error bounds. This work also provided the first attempt to validate the numerical models for the near-field dust emission and transport around a moving vehicle.

One unambiguous finding of literature review and our simulation studies was that current publicly available experimental data was inadequate to fully validate near-field dust emission and transport models. Most experimental data was commissioned to support atmospheric dust transport modeling for environmental quality impact studies. Basically these experimental studies were targeting data that is assumed to be averaged over time periods in the range of weeks to months, and over length scales on the order of kilometers or greater. As a result, most of these studies did not provide definitive data on the dust in the local area of the vehicle in the time-scale of a single traversal of a dusty terrain. Lacking detailed experimental data on the vehicle spatial and temporal scales, the ability to refine models beyond what was presented in this study is somewhat

limited: while more sophisticated modeling approaches could be suggested, there would be no way to provide sufficient validation of these models based on data available in the literature. Therefore, further enhancement of these models must proceed along with detailed experimental work focused on near-field measurement of fugitive dust emission on the appropriate time and space scales that would accurately capture localized dust behavior.

# 8 Acknowledgments

This work was supported by the U.S.Army TACOM Life Cycle Command under Contract No.W56HZV-08-C-0236, through a subcontract with Mississippi State University, and was performed for the Simulation Based Reliability and Safety (SimBRS) research program.

# References

[1] Gillies J, Etyemezian V, Kuhns H, Nikolic D, Gillette D. Effect of Vehicle Characteristic on Unpaved Road Dust Emissions. Atmos Environ. 2005;39:2341–2347.

[2] Gillies J, Etyemezian V, Kuhns H, Moosmueller H, Engelbrecht J, King J, et al. Particulate Matter Emissions Factors for Dust from Unique Military Activities. DRI; 2010. SERDP Project SI-1399.

[3] Veranth J, Pardyjak E, Seshadri G. Vehicle-Generated Fugitive Dust Transport: analytic models and field study. Atmos Environ. 2003;.

[4] Holsen T, Dhaniyala S, Hopke P. Fugitive Dust Emissions: Development of a Real-time Monitor. Clarkson University; 2011.

[5] Tsai CJ, Miaw DY. Emission Factor of Fugitive Dust From Paved Roads in Hsin Chu Taiwan. Journal of the Chinese Institute of Evironmental Engineering. 2001;11(4):245–252.

[6] EPA. Emission Factor Documentation for AP-42. US Environmental Protection Agency; 2003.

[7] EPA. Emission Factor Documentation for AP-42, Miscellaneous Source Chapter 13. US Environmental Protection Agency; 2003.

[8] Nickling W, Gillies J. Emission of Fine-Grained Particulate from Desert Soils. In: Sarnthein M, Leinen M, editors. Paleoclimatology and Paleometeorology: Modern and Past Patterns of Global Atmospheric Transport. Kluwer Academic Publisher, Dordrecht; 1989. .

[9] Shao Y, Raupach M, Findlater P. The Effect of Saltation Bombardment on the Entrainment of Dust by Wind. J of Geophys Res. 1993;p. 12719–12726.

[10] Gillies J, Arnott W, Etyemezian V, et al. Characterizing and Quantifying Local and Regional Particulate Matter Emissions From Department of Defense Installations. DRI and NASA and NDAA; 2005. SERDP Project CP-1191.

[11] DRI. SERDP Project SI-1400. Desert Research Institute; still active.

[12] EPA. Emission Factor Documentation for Ap-42, section 13.2.2, unpaved roads, final report. US Environmental Protection Agency; 1998.

[13] Chen J, Fu X, Wegman E. Real-Time Simulation of Dust Behavior Generated by a Fast Traveling Vehicle. ACM Transactions on Modeling and Computer Simulation. 1999;9(2):81–104.

[14] Chen J, Wegman E, Wang J. Animation of Dust Behaviors in a Networked Virtual Environment. In: 6th International Conference in Central Europ on Computer Gaphics and Visualization; 1998. p. 487–494.

[15] Mensink C, et al AC. Integrated Air Quality Modeling for the Assessment of Air Quality in Streets Against the Council Directives. Atmos Environ. 2003;37(37):5177–5184.

[16] Thomson D, Manning A. Along-wind Dispersion in Light Wind Conditions. Bound-Lay Meteorol. 2001;98(2):341–358.

[17] Stern R, Yamartino R. Development and First Evaluation of Micro-calgrid: a 3-D, Urban-canopy-scale Photochemical Model. Atmos Environ. 2001;35:149–165.

[18] Pasquill F. The Estimation of the Dispersion of Windborne Material. Meteorology Magazine. 1961;90:33–40.

[19] A Comparison of Calpuff Modeling Results to Two Tracer Field Experiments; 1998. Http://www.epa.gov/scram001/7thconf/calpuff/tracer.pdf.

[20] Wilcox DC. Turbulence Modeling for CFD. DCW Industries; 1998.

[21] Holmes N, Morawska L. A Review of Dispersion Modeling and its Application to the Dispersion of Particles: An Overview of Different Dispersion Models Available. Atmos Environ. 2006;40:5902–5928.

[22] Veluri S, Roy C, Luke E. Comprehensive Code Verification Techniques for Finite Volume CFD Codes. Computers and Fluids. 2012;70:59–72.

[23] Luke E, Cinnella P. Numerical Simulations of Mixtures of Fluids using Upwind Algorithms. Computers and Fluids. 2007;36:1547–1566.

[24] Zhang Y, Luke E. Concurrent Composition using Loci. Comput Sci Eng. 2009;11(3):27–35.

[25] Riddle A, Carruthers D, Sharp A, McHugh C, Stocker J. Comparisons between Fluent and ADMS for Atmospheric Dispersion Modeling. Atmos Environ. 2004;38:1029–1038.

[26] Walshe J. CFD Modeling of Wind Flow Over Complex and Rough Terrain (PHD disertation); 2003. University of Loughborough.

[27] Richards P, Norris S. Appropriate Boundary Conditions for Computational Wind Engineering Models Revisited. J Wind Eng Ind Aerodyn. 2011;99:257–266.

[28] Richards P, Hoxey R. Appropriate Boundary Conditions for Computational Wind Engineering Models Using the $k-\epsilon$ Turbulence Model. Journal of Wind Engineering and Industrial Aerodynamics. 1993;.

[29] Menter FR. Two-Equation Eddy-Viscosity Turbulence Models for Engineering Applications. AIAA Journal. 1994;32(8):1598–1605.

[30] Tong X, Luke E, Smith R. Sensitivity Studies on Particle Emissions and Transport Around a Moving Vehicle. In: NDIA Ground Vehicle Systems Engineering and Tehcnology Symposium. MSTV Mini-Symposium. Dearborn, Michigan: NDIA; 2011. .

[31] Wilson J. Turbulent Dispersion in the Atmospheric Surface Layer. Bound-Layer Meteor. 1982;22:399–420.

[32] Sawford B. Lagrangian Statistical Simulation of Concentration Mean and Fluctuation Fields. J Climate Appl Meteor. 1985;24:1152–1166.

[33] Thomson D. Criteria for the Selection of Stochastic Models of Particle Trajectories in Turbulent Flows. J Fluid Mech. 1987;180:529–556.

[34] Zannetti P. New Monte Carlo scheme for simulating Lagranian particle diffusion with wind shear effects. Appl Math Modell. 1984;8:188–192.

[35] Sethuraman S, Meyers R, Brown R. A Comparison of a Eulerian and a Lagrangian Time Scale for Over-Water Atmospheric Flows During Stable Conditions. Boundary-Layer Meteorology. 1978;14:557–565.

[36] Hanna S. Lagrangian and Eulerian Time-Scale Relation in the Daytime Boundary Layer. J of Appl Meteorol. 1980;.

[37] Kos I, Belusic D, Jericevic A, Horvath K, Koracin D, Prtenjak M. Education and Research: Initial Development of the Atmospheric Lagrangian Particle Stochastic (ALPS) Dispersion Model. GEOFIZIKA. 2004;21:37–52.

[38] Langston R, Merle Jr R, Etyemezian V, Kuhns H, Gillies J, Zhu D, et al. Clark County Paved Road Dust Emission Studies in Support of Mobile Monitoring Technologies. DAQEM and DRI and UC, Riverside and University of Neveda; 2003.

[39] Kuhns H, Gillies J, Etyemezian V, Nickolich G, King J, Zhu D, et al. Effect of Soil Type and Momentum on Unpaved Road Particulate Matter Emissions from Wheeled and Tracked Vehicles. Aerosol Sci Technol. 2010;p. 187–196.

[40] Nicholson K, Branson J, Geiss P, Channel R. The effects of Vehicle Activity on Particle Resuspension. J Aerosol Sci. 1989;20(1425-1428).

[41] Venkatram A. A Critique of Empirical Emission Factor Models: A Case Study of the AP-42 Model for Estimating $PM_{10}$ Emissions from Paved Roads. Atmos Environ. 2000;34:1–11.

[42] Marcum DL. Unstructured Grid Generation Using Automatic Point Insertion and Local Reconnection. In: The Handbook of Grid Generation. CRC Press; 1998. p. 1–18.

[43] Etyemezian V, Gillies J, Huhns H, Nikolic D, Watson J, Veranth J, et al. Field Testing and Evaluation of Dust Deposition and Removal Mechanisms: Final Report. DRI, Las Vegas, NV for the WESTAR Council, Lake Oswego, OR; 2003.